A Radiometer for a Space Communications Receiver

By E. A. OHM and W. W. SNELL

(Manuscript received March 28, 1963)

By adding a square wave of noise to the input of an ultra-low-noise receiver via a directional coupler, a radiometer with a sensitivity greater than a Dicke type can be achieved when the basic system temperature is less than 18°K. A noise-adding radiometer is compatible with a communications receiver and has been used (i) to measure and monitor the absolute system temperature and (ii) to check the boresighting of a space communications antenna by detecting and tracking radio stars.

I. INTRODUCTION

A noise-adding radiometer, unlike the Dicke type, does not require the input to be switched to a reference temperature. Since a typical good switch adds 7°K or more to the system temperature, it can cause a relatively large increase in the temperature of an ultra-low-noise receiver, and this in turn will cause a significant decrease in the radiometer and/or communications sensitivity. The use of an input switch can be avoided by using a noise-adding radiometer which, for an ultra-low-noise system temperature, is just as sensitive as a Dicke radiometer. A unique feature is that it can be added to an ultra-low-noise communications receiver without causing a large increase in the system temperature. Thus a sensitive tracking receiver, designed primarily to handle communications,[1] can also be used to monitor, measure, and map the system environment temperature including radio stars. Conversely, the radio stars with known positions can be used to check the boresighting of the antenna.

The major hardware components required for a noise-adding radiometer are readily available; the excess noise temperature, mismatch, and instability problems normally associated with a mechanical or ferrite switch are avoided; and the fluctuations due to imperfect circuit components can be reduced to an acceptable value by using a new high-

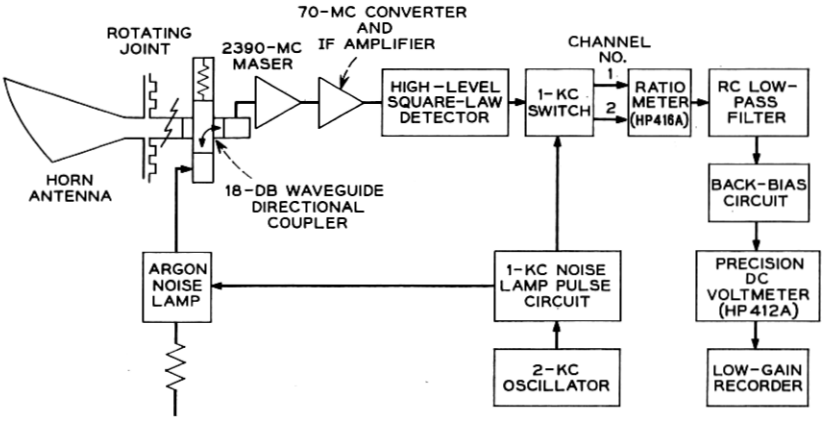

Fig. 1 — Block diagram of a noise-adding radiometer.

output-level square-law detector in combination with an improved noise lamp pulse circuit. In particular, a threshold of $\Delta T = 0.04°\text{K}$ ($2\frac{1}{2}$ times theoretical) has been achieved for periods of 10 seconds when the post-detection time constant is 1 second. For 30-minute periods, a long-term threshold of $\Delta T = 0.12°\text{K}$ (10 times theoretical) has been achieved when the time constant is 15 seconds. Due to the rather small aperture of the Crawford Hill horn-reflector antenna, 26.8 square meters, the corresponding long-term flux or power density threshold is 1.2×10^{-25} watts meter^{-2} cps^{-1}, but this is sufficiently sensitive to detect and track 30 or more radio stars as well as Venus near inferior conjunction. Cassiopeia A and Virgo A have been measured and found to have flux densities of 1.47×10^{-23} and 1.48×10^{-24} watts meter^{-2} cps^{-1}, respectively, at 2390 mc. The uncertainty of measurement is less than 15 per cent. Since absolute system temperatures can be rapidly and precisely recorded for many hours at a time, it was also practical to obtain data for, and prepare, an accurate environment temperature map of the horn antenna site at Crawford Hill, New Jersey.

A block diagram of the noise-adding radiometer is shown in Fig. 1. In the manual mode of operation, a known amount of excess noise from an argon noise lamp is added to the input circuit via a waveguide directional coupler. This gives a ratio, Y, of the system input temperature with the noise added, $T_S + T_A$, to the system input temperature, T_S.

$$Y = \frac{T_S + T_A}{T_S} \tag{1}$$

therefore

$$T_S = \frac{T_A}{Y - 1}. \tag{2}$$

To determine T_S, Y can be measured by noting the change in IF attenuation required to keep the IF output power constant when the noise lamp is turned on. Alternatively, since the detector is square-law and the IF amplifier is linear, Y is also given by the ratio of the output voltages of the square-law detector. Since the first method is more accurate, it serves as a calibration check for the second, which is more suitable for a continuous measurement.

The ratio of output voltage, Y, is generated a thousand times per second by pulsing the noise lamp at a 1-kc (50 per cent duty cycle) rate. This produces a rectangular wave at the output of the square-law detector as shown in Fig. 2. The rectangular wave is then passed through a solid-state single-pole, double-throw switch, also operated at 1 kc, where the voltage proportional to $T_S + T_A$ is always switched to channel 1, and the voltage proportional to T_S is always switched to channel 2. The two waveforms are filtered to obtain the fundamental 1-kc components and are then connected in-phase to a ratio-meter. The ratio, Y, is continuously indicated on a calibrated meter, and also by the output voltage of the ratio-meter. Since T_S is a function of Y and the known constant T_A, (2), the continuous outputs can be readily calibrated in terms of the absolute system temperature.

A small change in input temperature can be measured with good accuracy by using observed values of Y and ΔY. Differentiating (2)

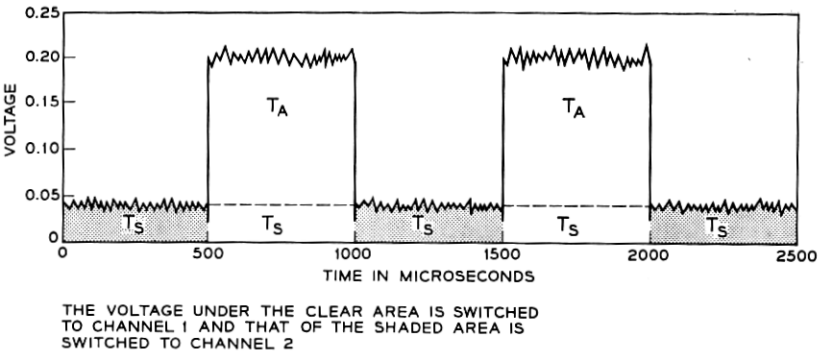

Fig. 2 — Output voltage of a square-law detector.

$$\frac{dT_S}{dY} = -\frac{T_A}{(Y-1)^2}.$$

Substituting T_S of (2) for $T_A/(Y-1)$

$$\Delta T_S = -\frac{T_S}{Y-1}\Delta Y \tag{3}$$

where T_S, Y, and ΔY can be found from the output voltages of the ratio-meter.

II. MINIMUM DETECTABLE CHANGE OF INPUT TEMPERATURE

It is shown in Appendix A that the theoretical minimum change of input temperature which causes the output voltage, V, to change the same amount as the rms value of the noise fluctuation is

$$\Delta T_S \text{ (theoretical)} = T_S\left(1+\frac{T_S}{T_A}\right)\frac{\pi}{2}\frac{1}{\sqrt{B\tau}} \tag{4}$$

where: T_S = the total system temperature referred to the waveguide input
T_A = the temperature added when the noise lamp is on
B = the IF (predetection) bandwidth
τ = the RC time constant of the output (post-detection) filter.

Although it may appear anomalous that ΔT_S is reduced as T_A is increased, this can be explained in terms of the relative amplitude of the 1-kc rectangular wave in channel 1 compared to that in channel 2. Referring now to Fig. 2, an increase in system temperature will increase the amplitude of each 1-kc component the same amount. If one is much larger than the other, however, the percentage decrease in ratio, Y, will be larger, and this in turn will cause a larger change in the output voltage of the ratio-meter. At the same time, the theory of a square-law detector shows that the fluctuation in each channel due to noise power is proportional to the 1-kc signal power. Thus the signal-to-noise ratio in each channel is independent of the amplitude of the 1-kc rectangular wave. It follows that the signal-to-noise ratio at the output of the ratio-meter is also independent of the input amplitudes. Since the output signal voltage due to a change in system temperature has been enhanced, and the output signal-to-noise ratio is unchanged, it is thus possible to detect a smaller signal when the 1-kc rectangular waves have a larger difference in amplitude. In this application, the difference is achieved by adding noise T_A to channel 1.

In the limit, T_A and the amplitude of channel 1 are infinite. In this case a change in system temperature cannot affect the amplitude of channel 1, and it can be considered as a reference. Since the radiometer is now insensitive to the system temperature for half the time, it operates in the limit as a Dicke radiometer. For comparison, the sensitivity of a Dicke radiometer is discussed later in connection with (15). A tentative comparison of (15) to (4) with $T_A \to \infty$ shows that *if* the system temperatures could be made equal, the sensitivities would also be equal.

Since T_A cannot be made infinite, its value must be taken into account when calculating the sensitivity of a noise-adding radiometer. In particular, T_A can be altered over a wide range by changing the coupling, L, of the directional coupler, i.e.,

$$T_A = L\,T_H \tag{5}$$

where T_H is the excess noise available from the noise lamp. When the noise lamp is off, the coupling L also adds room temperature noise from the noise lamp termination to the basic system temperature

$$T_S = T_{\text{basic}} + T_{\text{room}}\,L = T_{\text{basic}} + 290L. \tag{6}$$

Thus T_S will also be altered over a wide range. Upon substitution of (5) and (6) into (4)

$$\Delta T_S(\text{theoretical}) = \left\{(T_{\text{basic}} + 290L) + \frac{(T_{\text{basic}} + 290L)^2}{LT_H}\right\}\frac{\pi}{2}\frac{1}{\sqrt{B\tau}}. \tag{7}$$

By differentiating (7) with respect to L and setting the result equal to zero, it can be shown that (7) has an optimum minimum when L has the value

$$L(\text{optimum}) = \frac{T_{\text{basic}}}{(290)^{\frac{1}{2}}(T_H + 290)^{\frac{1}{2}}}. \tag{8}$$

Substituting back into (7)

$$\Delta T_S(\text{optimum}) \approx \left[1 + 2\left(\frac{290}{T_H}\right)^{\frac{1}{2}} + 2\left(\frac{290}{T_H}\right) + \left(\frac{290}{T_H}\right)^{\frac{3}{2}}\right]\frac{\pi}{2}\frac{T_{\text{basic}}}{\sqrt{B\tau}}. \tag{9}$$

For a practical value of T_H, 10,200°K,[2] (9) reduces to

$$\Delta T_S(\text{optimum}) = 1.4\,\frac{\pi}{2}\frac{T_{\text{basic}}}{\sqrt{B\tau}}. \tag{10}$$

For a communications receiver, it is desirable to minimize L of (6) and have T_S as close as practical to T_{basic}. Using (6) and (8):

$$\frac{T_S}{T_{\text{basic}}} = 1 + \frac{290L}{T_{\text{basic}}} = 1 + \frac{L}{L(\text{optimum})}\left(\frac{290}{T_H + 290}\right)^{\frac{1}{2}}. \quad (11)$$

For $L = L(\text{optimum})$ and $T_H = 10{,}200°\text{K}$, T_S is 16.6 per cent larger than T_{basic}. For $L = \frac{1}{4} \times L(\text{optimum})$ this can be reduced to a more acceptable 4.2 per cent. By substituting $L = \frac{1}{4} \times L(\text{optimum})$ into (7) and comparing the result with that of (9), it can be shown that ΔT_S-(theoretical) is increased 35 per cent. Since ΔT_S(theoretical) is equivalent to the theoretical rms value of noise fluctuation, and since it has been found that other practical sources of fluctuation add $1\frac{1}{2}$ times as much to this value, the percentage increase in ΔT_S(total) due to an increase in ΔT_S(theoretical) is reduced by a factor of $2\frac{1}{2}$. Thus, in practice, the total fluctuation is increased only about 14 per cent. Since this is an acceptable penalty, the recommended value of L is

$$L(\text{for communications receiver}) = \tfrac{1}{4} \times L(\text{optimum}).$$

For the nonoptimum values of T_H and L used here, along with the values of other parameters encountered in the experiment, i.e., for

$$\begin{aligned} T_H &= 6190°\text{K}^* \\ L &= 0.0153(-18.15\text{ db}) \\ T_A &= L\,T_H = 94.6°\text{K} \\ T_S &= 21.0°\text{K (at the zenith)} \\ 290L &= 4.45°\text{K} \\ T_{\text{basic}} &= T_S - 290L = 16.55°\text{K} \\ B &= 7.75\text{ mc} \\ \tau &= 1\text{ sec.} \end{aligned}$$

The nonoptimum theoretical value of ΔT_S can be found by inserting the values of T_S and T_A in (4) which, for convenience, can be written

$$\Delta T_S(\text{theoretical}) = \frac{T_S}{T_{\text{basic}}}\left(1 + \frac{T_S}{T_A}\right)\frac{\pi}{2}\frac{T_{\text{basic}}}{\sqrt{B\tau}} = 1.55\,\frac{\pi}{2}\frac{T_{\text{basic}}}{\sqrt{B\tau}}. \quad (12)$$

Comparison of (12) and (10) shows that the theoretical threshold

* T_H was relatively small since it came from a coaxial noise lamp and was further reduced by a coaxial line loss. See p. 1087 of Ref. 1.

sensitivity with the above experimental parameters is only 10 per cent less than optimum.* By inserting experimental values for T_{basic} and B in (12), the corresponding numerical value of ΔT_S is

$$\Delta T_S(\text{theoretical}) = 0.015°\text{K} \tag{13}$$

when the post-detection time constant, τ, is one second.

III. COMPARISON WITH A DICKE RADIOMETER

An expression for the threshold sensitivity of a Dicke[3] radiometer in which only one RF sideband is contributing to the receiver output has been worked out in similar terms by Selove.[4] His analysis assumes that the switched reference temperature is small compared to the over-all system temperature. To be valid for an ultra-low-noise receiver, it must be assumed that the switched reference temperature is very low and about equal to the antenna-plus-sky temperature. It is not at room temperature as in the original Dicke radiometer. Thus, from the first two paragraphs of Selove's Appendix,

$$\frac{\Delta T_S}{T_S} = \pi \sqrt{\frac{b}{B}} \tag{14}$$

where: b = the output low-pass-filter (post-detection) bandwidth, and B = the IF (pre-detection) bandwidth. On writing $b = \frac{1}{4}\text{RC} = 1/4\tau$, i.e., in terms of the time constant of an equivalent noise bandwidth, the threshold temperature is

$$\Delta T_S(\text{Dicke}) = T_S \frac{\pi}{2} \frac{1}{\sqrt{B\tau}} \tag{15}$$

where T_S, in this case, is composed of the basic system temperature plus the temperature added by the required input switch.

$$T_S = T_{\text{basic}} + T_{\text{switch}} .$$

The effect of T_{switch} on the sensitivity can be seen by putting (15) in the form

$$\Delta T_S(\text{Dicke}) = \left(1 + \frac{T_{\text{switch}}}{T_{\text{basic}}}\right) \frac{\pi}{2} \frac{T_{\text{basic}}}{\sqrt{B\tau}} .$$

From comparison with the threshold temperature of an optimized noise-adding radiometer, (10),

* For the value of T_H used here and the observed value of T_{basic}, L is very close to the optimum value called for by (8). Thus nearly all the reduction in sensitivity is due to the relatively small value of T_H.

$$\frac{\Delta T_s(\text{Dicke})}{\Delta T_s(\text{noise-adding})} = \left(\frac{1 + (T_{\text{switch}}/T_{\text{basic}})}{1.4}\right). \tag{16}$$

Thus, when $T_{\text{switch}} \ll T_{\text{basic}}$, the threshold temperature of a noise-adding radiometer is 40 per cent greater than that of the Dicke radiometer. However, the threshold temperature will be less; i.e., the noise-adding radiometer will be more sensitive, if $T_{\text{basic}} < 2.5T_{\text{switch}}$. Since a practical input waveguide switch has an insertion loss of 0.1 db or more, a typical value of T_{switch} is at least 7°K. Thus, if the basic system temperature is 18°K or less, an optimized noise-adding radiometer can be more sensitive than a Dicke radiometer. Since the over-all sensitivity in each case is determined largely by fluctuations added by the required practical circuits, and since the circuits for each radiometer are different, the theoretical comparison at this time merely indicates that the over-all sensitivities are similar.

IV. MINIMUM DETECTABLE POWER DENSITY

Although the sensitivity of a radiometer can be conveniently expressed in terms of ΔT_s, the more important system parameter is the minimum detectable change of power density per cycle of bandwidth. It will now be shown how these are related by the effective area of the antenna. To start,

$$P_{\text{received}} = \tfrac{1}{2} \times P \times A$$

where: P = the incident power flow in watts per square meter, and A = the effective antenna area in square meters. The factor $\frac{1}{2}$ allows for the fact that the receiver is sensitive to only a single polarization. Solving for P,

$$P = \frac{2}{A} \times P_{\text{received}} = \frac{2}{A} KT_sB$$

where: K = Boltzmann's constant, B = the bandwidth in cycles per second, and T_s = the equivalent input temperature. The incident power flow per cycle of bandwidth is therefore

$$\frac{P}{B} = \frac{2K}{A} T_s. \tag{17}$$

In the radio astronomy literature, the quantity P/B is often called the flux density, S. Small changes in flux density, ΔS, are proportional to changes in the input temperature, ΔT_s, and therefore,

$$\Delta S = \Delta\left(\frac{P}{B}\right) = \frac{2K}{A} \Delta T_s. \tag{18}$$

Upon substitution of numerical values for K, 1.380×10^{-23} joules/degree, and A, 26.8 square meters at 2390 mc,[5]

$$\Delta S = 1.02 \times 10^{-24} \times \Delta T_s . \tag{19}$$

Upon further substitution of the minimum detectable change of input temperature, 0.015°K from (13), the minimum detectable change in flux density, for $\tau = 1$ second, is

$$\Delta S(\text{theoretical}) = 1.53 \times 10^{-26} \text{ watts meter}^{-2} (\text{cps})^{-1} \tag{20}$$

The experimental value of ΔS is somewhat larger, and the increase is due to other sources of system temperature fluctuation, which will be identified and discussed in the following description of the radiometer parts.

V. COMMUNICATIONS RECEIVER

The Echo receiver had an over-all system temperature of 21.0°K,[1] and its steerable horn-reflector antenna provided an effective area of 26.8 square meters.[5] The area is rather small for observing point-source radio stars, but the disadvantage is compensated, in part, by the small contribution to the system temperature by the far-side and back lobes of a horn-reflector antenna. This minimizes the random change in system temperature as the antenna beam is moved, and this in turn allows (*i*) tracking to achieve a longer observation time and (*ii*) lobing to obtain a more accurate position measurement.

The antenna is connected to the maser package with about 5 feet of assorted waveguide. Included is a rotating joint for mechanically decoupling the antenna from the receiver and a 18.15-db directional coupler for adding noise from a noise lamp. Of the 21.0°K system temperature, about 2.5°K is due to the loss and temperature of the waveguide and 4.5°K is due to the room temperature termination of the directional coupler. Of the 8°K added by the maser package, about 7°K is believed due to the near-room-temperature insertion loss of the input coaxial line.[6] Thus, about 14°K of the system temperature is proportional to room temperature and as such is a source of long-term fluctuation.

$$\Delta T_{SR} = 14 \times \frac{\Delta T(\text{room})}{T(\text{room})} . \tag{21}$$

For $T = 290$°K and an observed value of $\Delta T(\text{room}) = \pm 1$°K, due to air conditioner cycling, the calculated rms value of ΔT_{SR} is 0.034°K. However, the waveguide and coaxial lines have a poor thermal contact

with the air and thus a long thermal time constant. Although the period of air conditioner cycling depends on the weather, it is usually relatively short, and therefore the actual value of ΔT_{SR}, in general, will be somewhat less. A typical value is probably about 0.02°K.

In regard to the rotating joint, a gap of 20 mils or less, and an offset error of 15 mils or less,[1] were sufficient to reduce this source of temperature fluctuation to a trivial amount.

A balanced diode converter follows the maser amplifier and contributes a small amount of noise, T_{sc}, to the system temperature

$$T_{sc} = \frac{T_{\text{converter}}}{G_{\text{maser}}} = \frac{2700°K^*}{4000\ (36\,\text{db})} = 0.68°K. \tag{22}$$

T_{sc} will change, however, if either the maser gain or the converter temperature changes. Taking the total differential

$$\Delta T_{sc} = T_{sc}\left(\frac{\Delta T_c}{T_c}\right) - T_{sc}\left(\frac{\Delta G_m}{G_m}\right)$$

where: $\Delta T_c/T_c$ = the estimated change in normalized converter temperature in 30 minutes = ± 0.01

$\Delta G_m/G_m$ = the measured change in normalized maser gain in 30 minutes = ± 0.045.

Assuming that ΔT_c and ΔG_m are statistically independent

$$\Delta T_{sc} = T_{sc}\left[\left(\frac{\Delta T_c}{T_c}\right)^2 + \left(\frac{\Delta G_m}{G_m}\right)^2\right]^{\frac{1}{2}}. \tag{23}$$

Upon substitution of the numerical values, ΔT_{sc} (rms value) = 0.022°K. This source of fluctuation can be nearly eliminated, i.e., T_{sc} can be reduced toward zero, by using a maser with a larger gain or by using two masers in series.

A net gain of 116 db is provided to drive the high-level square-law detector with an IF noise power of +6 dbm when the noise lamp is on. This is 12 db under the maximum linear IF output power and provides a safe margin for the higher noise peaks. The predetection bandwidth, B, of the radiometer is limited by the converter preamplifier to 7.75 mc. If this is increased to 16 mc, the maser bandwidth, the theoretical sensitivity, from (4), could be increased by a factor of $1\frac{1}{2}$.

VI. HIGH-OUTPUT-LEVEL SQUARE-LAW DETECTOR

By detecting a high-output level of voltage, the separate channel gains which follow the 1-kc switch can be reduced to a minimum. Since

* The interconnecting cable loss, 2.3 db, is included as part of this temperature.

the gains can vary independently and thus increase the system fluctuation, they can and should be reduced to a minimum. The square-law characteristic is needed to convert the IF power, which is proportional to the input temperature, to a linear output voltage. The combination of high-output level and square-law is usually difficult to obtain, but has been achieved with the circuit shown in Fig. 3. As indicated, a relatively high output voltage, 0.5 volt, can be generated by a network of series-parallel diodes when the available input power is +7.5 dbm. For expediency, the detector assembly was matched to the output im-

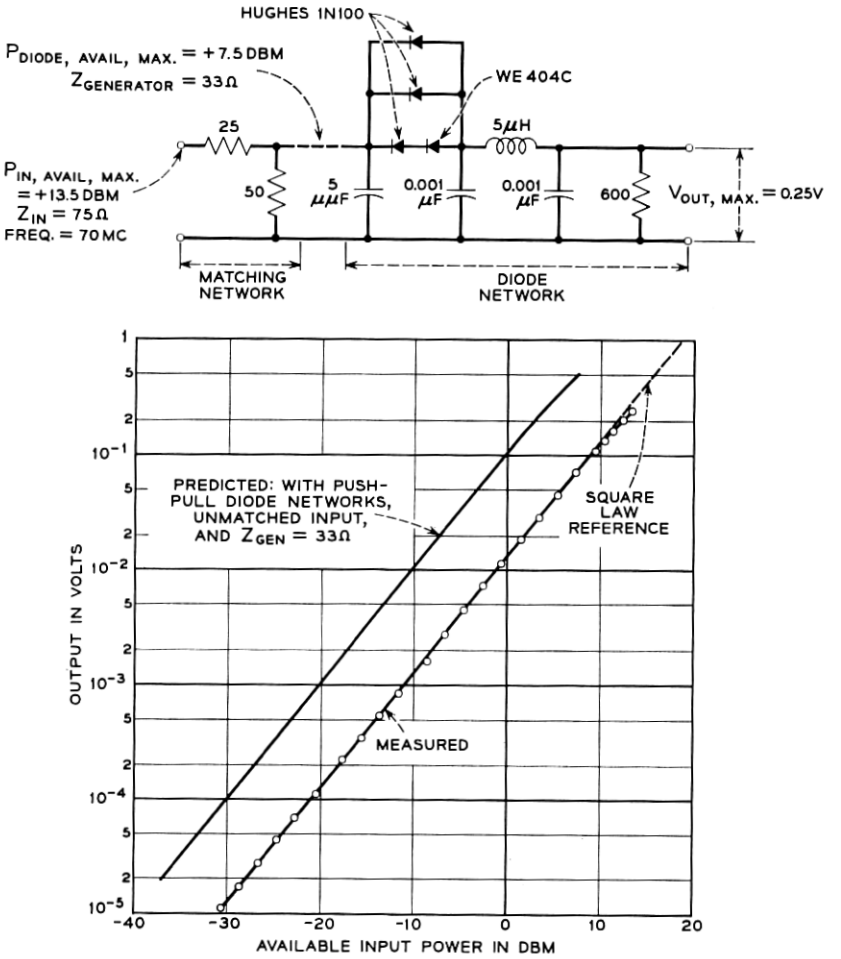

Fig. 3 — Characteristics of a high-output-level square-law detector.

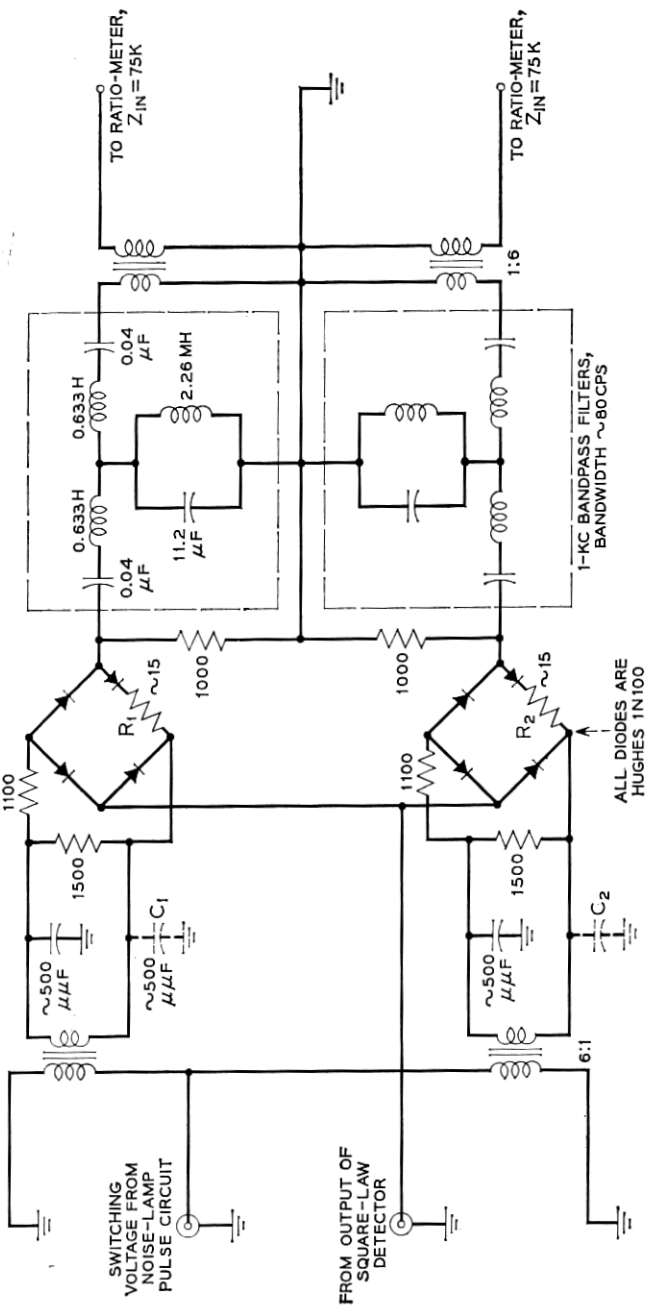

Fig. 4 — One-ke diode switch assembly.

pedance of the IF amplifier, and the required low impedance for driving the diode network was obtained, by using a resistive matching network. The measured characteristic is shown by the lower curve of Fig. 3. It was experimentally verified that the output voltage can be doubled for a given available diode drive power by placing a second diode network of reversed polarity in parallel with the first. Since the insertion loss of the resistive matching network is 6 db, and it can be replaced by a lossless reactive network with the same generator impedance, the doubled output voltage can be achieved with a 6-db reduction in the available input power. The anticipated characteristic is indicated by the upper curve of Fig. 3. For a precision square-law application, the output voltage of a single-ended diode network should not exceed 0.125 volt, and that of a push-pull diode network should not exceed 0.25 volt. The corresponding available input power, from the upper curve of Fig. 3, can then be as low as +4 dbm. Since the maximum linear IF noise power output is +6 dbm, and the circuit of Fig. 3 was used in the experimental radiometer, the corresponding output voltage, from the lower curve of Fig. 3, was on the order of 0.05 volt.

VII. DIODE SWITCH ASSEMBLY

The diode switch assembly consists of two clusters of Hughes 1N100 diodes, each forming a bridge network as shown in Fig. 4. The two bridge networks are energized 180° out of phase and receive a 1-kc switching voltage, a 15-volt, peak-to-peak square wave, from the noise lamp pulse circuit. The switching voltage is isolated from the input and output circuits by the balance resistors R_1, R_2 and capacitors C_1, C_2. Since the isolation tuning is a function of particular diode impedances and driving transformer capacitances (to ground), the values shown are nominal. By potting the diodes in an insulating compound, it has been possible to reduce the system fluctuation due to thermal changes to a negligible amount.*

VIII. RATIO-METER

A ratio-meter (Hewlett Packard 416A) is used to measure the ratio of the sinusoidal voltage amplitudes supplied by the 1-kc switch assembly. One output for indicating the ratio, Y, is a meter on the front

* The diodes are switched continuously, even when the noise lamp is off, in order to provide 1-kc reference signals for the ratio-meter when $Y = 1$. This also improves the long-term stability since possible diode heating, due to switching power, is held constant.

panel. From the theory of operation,[7] the differential voltage across the meter is

$$V_{\text{meter}} \approx C \times \tan^{-1}(1/Y). \tag{24}$$

To take nonlinearities into account, the meter face must be calibrated, and one of the factory calibrated scales, Percent Reflection, is equal to $100\sqrt{1/Y}$. Thus, in principle, Y can be derived from this scale. In practice, however, the ratio indicated by the meter may be somewhat less than the true value due to ignition and deionization times associated with the noise lamp. Therefore, the meter was recalibrated, as discussed in Appendix B, for measured values of Y, and a typical result is shown in Fig. 5.

The other output for indicating Y is a single-ended voltage similar in form to (24)

$$V_{\text{out}} \approx 6 \times \tan^{-1}(1/Y). \tag{25}$$

In order to reduce error due to loading by the measuring and recording circuit, a cathode follower was added as shown in Fig. 6, and its output, V, was used as the ratio-meter output voltage. V was calibrated for measured values of Y, as discussed in Appendix B, and a typical result is shown by the upper left-hand curve of Fig. 7. The corresponding locus of T_S was calculated from (2) for the experimental value of T_A, i.e., 94.6°K.

Thus, from Fig. 7, the absolute system temperature, T_S, can be found by measuring the ratio-meter output voltage. In addition, small changes in system temperature, ΔT_S, can be found by measuring V and ΔV and using these in connection with (3)

$$\Delta T_S = \frac{-T_S}{Y-1}\Delta Y = \frac{-T_S}{Y-1}\frac{\Delta Y}{\Delta V}\Delta V \tag{26}$$

where T_S, Y, and $\Delta Y/\Delta V$ are functions of V and can be found from Fig. 7. For $T_S = 21.0°K$, (26) reduces to

$$\Delta T_S = 12.5 \times \Delta V. \tag{27}$$

The ratio-meter offers good discrimination against a change in RF or IF gain. From the accuracy specification, it can be shown that a change of 1 db will change the output voltage about 0.00001 volt. Upon substitution in (27), the apparent change in system temperature (rms value) is $\Delta T_{SG} = 0.001°\text{K}$. Since this is an order of magnitude less than the minimum detectable signal given by (13), this source of fluctuation can be neglected. Other sources affected the ratio-meter, how-

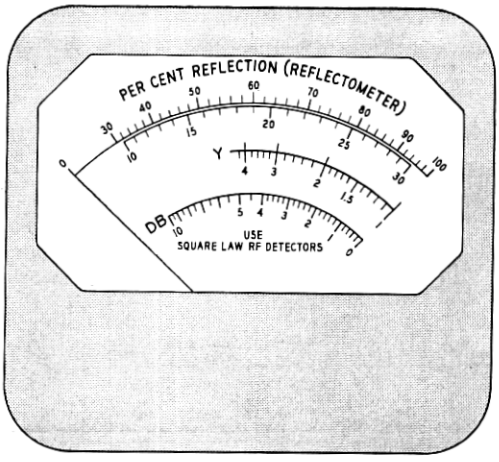

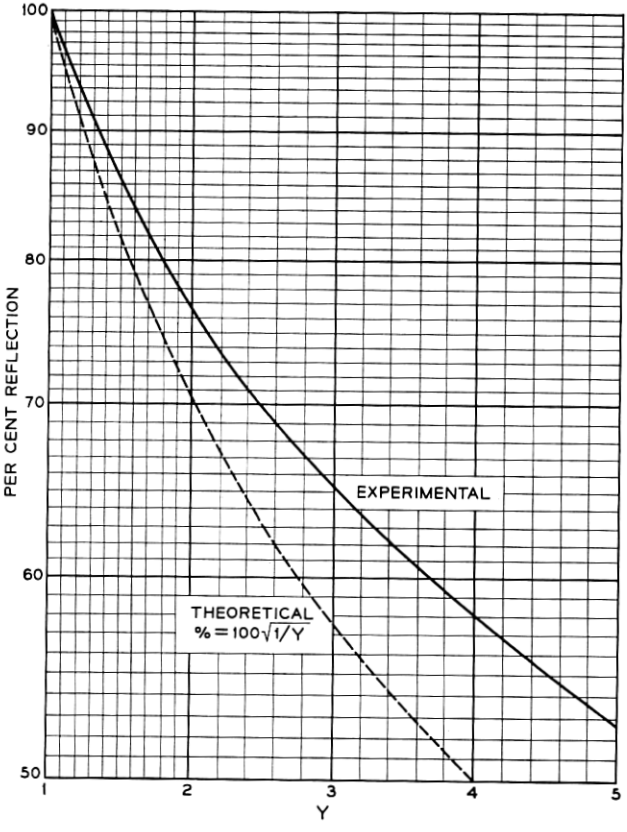

Fig. 5 — A typical ratio-meter "meter" calibration.

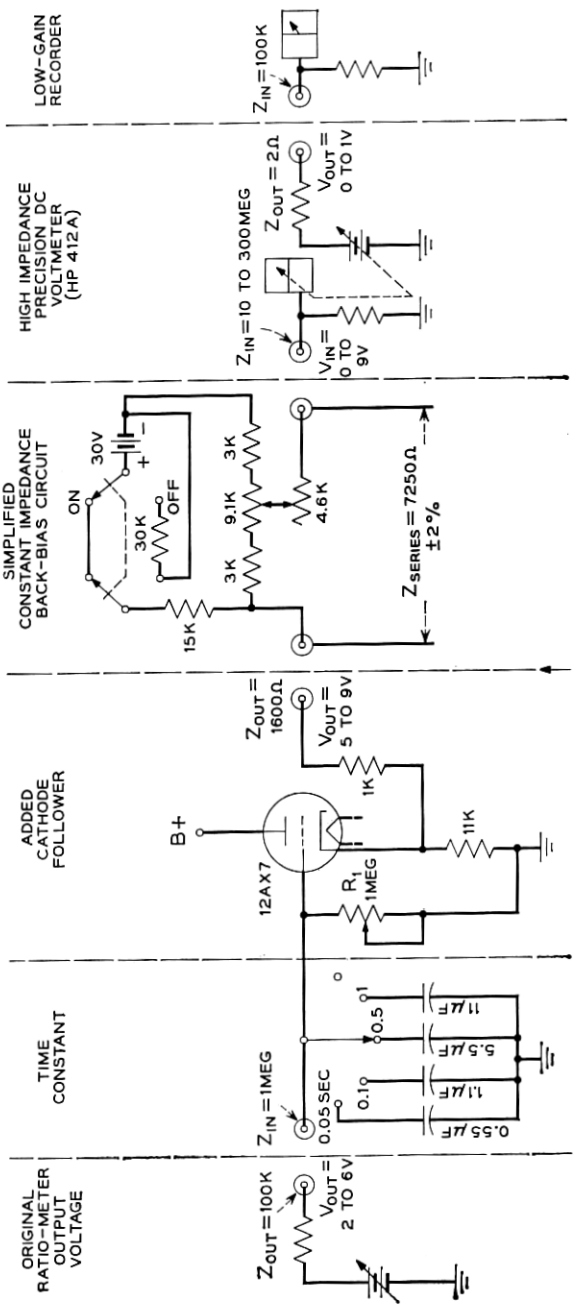

Fig. 6 — Measuring and recording circuit.

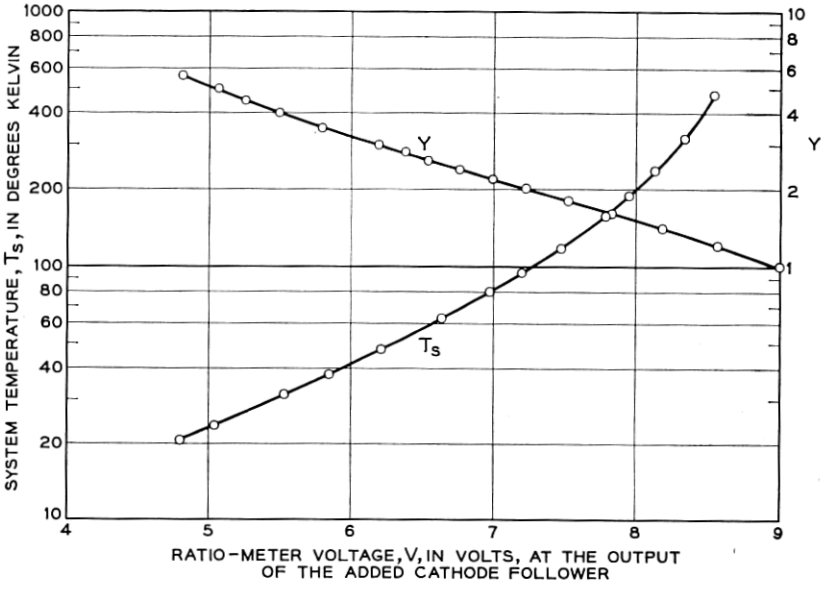

Fig. 7 — Typical ratio-meter voltage calibrations.

ever, and generated relatively large fluctuations, equivalent to 0.5°K. These were traced to changes in line voltage, vibration, and changes in room temperature, and were reduced by (*i*) regulating the line voltage and supplying the filaments with a regulated dc voltage, (*ii*) substituting premium tubes for the standard factory-supplied tubes, and (*iii*) placing the ratio-meter in an oven with a controlled temperature of 105°F. With these modifications, the fluctuations coming from the ratio-meter were reduced to

$$\Delta T_{SR} = 0.015°\text{K (short-term)}$$
$$= 0.04°\text{K (long-term)}.$$

The short-term fluctuation is an rms value observed over periods of 10 seconds, and the long-term fluctuation is an additional rms value observed over periods of 30 minutes. Separate channel gains are built into a commerical ratio-meter to allow for low input voltages and to provide for a large dynamic range. Since large voltages are available from a square-law detector, and since the dynamic range required in this application is relatively small, the separate channel gains are not needed and should be reduced and/or eliminated. It is believed that this modi-

fication will cause a further significant decrease in the long- and short-term fluctuations contributed by the ratio-meter.

IX. MEASURING AND RECORDING CIRCUIT

The voltage range to be measured and recorded is indicated by the abscissa of Fig. 7. To estimate the required order of stability, the value of ΔV which corresponds to the threshold value of ΔT_S can be found from (26). Solving for ΔV

$$\Delta V = -\frac{Y - 1}{T_S}\frac{\Delta V}{\Delta Y}\Delta T_S . \tag{28}$$

Upon substitution of $\Delta T_S = 0.015°\text{K}$ from (13), $T_S = 21.0°\text{K}$, and the values of Y and $\Delta V/\Delta Y$ from Fig. 7 which correspond to $T_S = 21.0°\text{K}$, the threshold value of ΔV is 0.0012 volt. In order to measure this change in voltage, a back-bias circuit is needed to buck out the 5 to 9 volts dc; a sensitive dc meter is needed; and the utmost stability is required. These objectives were met by combining a constant impedance back-bias circuit with a precision high-impedance voltmeter (Hewlett-Packard 412A), as shown in Fig. 6.

In regard to the back-bias circuit, note that V, in contrast to ΔV, can be readily measured with the precision voltmeter by turning off the back-bias switch. When this is done, the series impedance (7250 ohms) and the battery drain (1 ma) are both held constant to maintain good stability.

The voltage finally recorded is generated by the precision voltmeter. Since it varies from 0 to 1 volt for any full-scale meter deflection, a low-gain and therefore stable recorder can be used. Since the precision voltmeter drift is less than 0.1 per cent on any scale, and since the drift in back-bias voltage is less than 0.0001 volt, the total fluctuation due to the measuring and recording circuit is negligible.

X. NOISE LAMP PULSE CIRCUIT

The circuit outlined in Figs. 8 and 9 can be used to operate a fluorescent or argon gas discharge tube with a near 50 per cent duty cycle and a repetition frequency from 40 to 2000 cps. The excess noise is very stable; the on current can be varied over a wide range; and the filament is expected to last as long as it would in continuous service. In this application the repetition frequency was adjusted to coincide with the 1-kc center frequency of the ratio-meter.

The key to a stable pulsed noise output is that the high-voltage igni-

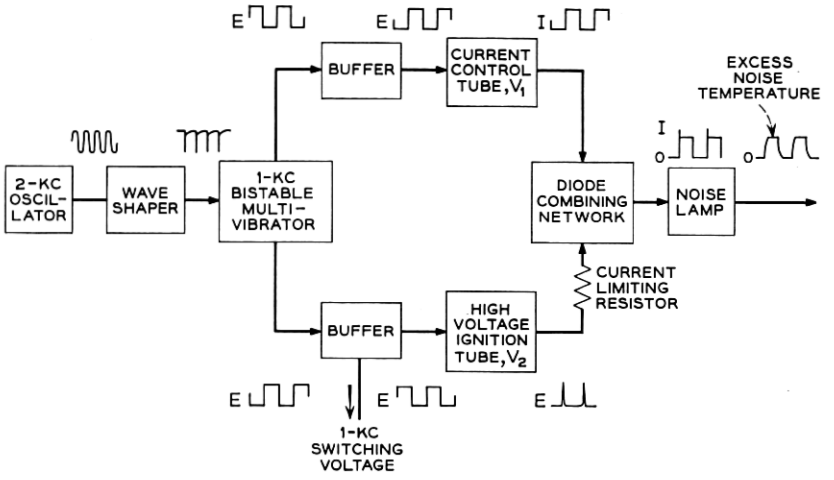

Fig. 8 — Block diagram of an improved noise lamp pulse circuit.

tion spike is generated in parallel with, rather than in series with, the main current path, and it is applied to the noise lamp via a large series resistance. Referring to Fig. 9, the sequence of operation is: (*i*) V_2 is initially conducting and its current stores magnetic energy in the inductance, L_1. V_1 is cut-off. (*ii*) To achieve ignition, V_2 is now cut-off and V_1 is biased into conduction. The slow collapse of the magnetic field maintains a near-constant current, which, since V_2 is cut-off, increases

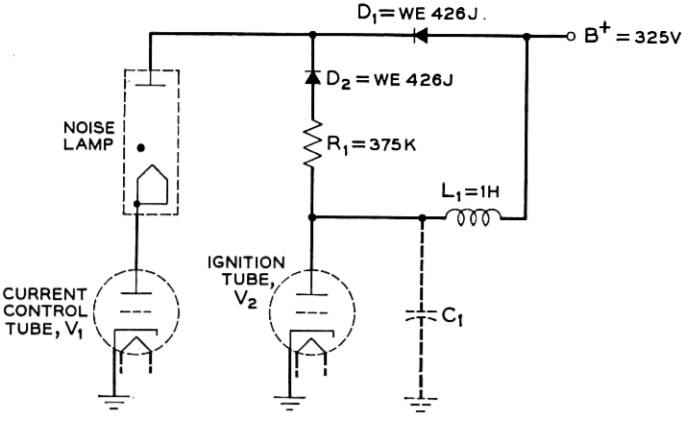

Fig. 9 — Critical parts of an improved noise lamp pulse circuit.

the voltage across C_1 towards a very large value. C_1, incidentally, is due primarily to the stray capacitance associated with L_1. Since the deionized noise lamp has an infinite resistance and since its anode is isolated from $B+$ by diode D_1, the rising voltage of C_1 is also applied across the noise lamp. (*iii*) When sufficient voltage is developed, the noise lamp is ionized and its resistance falls abruptly to 375 ohms. In a conventional circuit in which the anode of the noise lamp is connected to the junction of L_1 and C_1, the charge stored in C_1 is discharged directly through the noise lamp via V_1. This causes an undesirable high-power transient, which in turn causes severe ionic bombardment of the noise lamp filament. In the circuit of Fig. 9, however, the charge stored in C_1 is largely dissipated in the current-limiting resistor, R_1. (*iv*) After ionization, the current control tube, V_1, allows an adjustable amount of current to flow for the rest of the on period via the diode D_1. (*v*) At the beginning of the off period, V_1 is again biased beyond cut-off and V_2 is biased into conduction. This is the initial condition and the sequence is repeated at the start of the next on period.

By accounting for all other output voltage variations, it was estimated that the short-term (10-second) fluctuation at the ratio-meter output due to the noise lamp and its pulse circuit was $\Delta V \approx 0.0008$ volt (rms), and the additional long-term (30-minute) variation was $\Delta V \approx 0.0020$ volt (rms). The equivalent rms changes in system temperature, from (27), are

$$\Delta T_{SL} = 0.010°\text{K (short-term)}$$

$$= 0.025°\text{K (long-term)}.$$

Incidentally, the corresponding change in noise lamp temperature, ΔT_H, can be found by substituting $(T_S + T_A)/T_S$ for Y in (25), and then differentiating with respect to T_A. After rearranging,

$$\Delta T_A = -\frac{(T_A + T_S)^2 + T_S^2}{6T_S}\Delta V.$$

Since ΔT_A is attenuated from ΔT_H by the waveguide directional coupling, L, and by the transmission coefficient, K, of the coaxial line connecting the noise lamp to the directional coupler,

$$\Delta T_H = -\frac{(T_A + T_S)^2 + T_S^2}{6T_SKL}\Delta V. \tag{29}$$

For $K = 0.73$ and the experimental values of T_A, T_S and L, the change

in noise lamp temperature is

$$\Delta T_H = 9900\ \Delta V.$$

For the estimated total value of ΔV, 0.0028 volt (rms), the apparent value of ΔT_H (rms) is only 28°K, i.e., very small compared to T_H = 6190°K.

It is shown by (36) of Appendix A that the ratio-meter, to a first order, responds to only the in-phase component of the 1-kc input voltages. By assuming a model of flat-topped and delayed excess noise, it can further be shown, using Fourier analysis, that the difference between the experimental and theoretical calibration curves, Fig. 5, can be explained by an ionization delay of 160 microseconds and a deionization lag of 64 microseconds. For comparison, the desired excess noise interval is 500 microseconds. The calculated delays are similar to those reported by Kuhn and Negrete.[8] Thus the excess noise is apparently delayed into the off time interval and, in addition, it is on for only 404 microseconds. By delaying the 1-kc switching voltage of Fig. 8 about 110 microseconds, T_A can be centered in the on time slot with a guard time of 50 microseconds on either edge. An analysis of this shows that the experimental calibration curve, Fig. 5, will then be within $\frac{1}{2}$ division of the theoretical. The improvement in timing is highly recommended since it will probably eliminate most of the fluctuations attributed to the noise lamp pulse circuit.

XI. SUMMARY OF FLUCTUATIONS

The system fluctuations, in terms of rms changes in system temperature, are summarized in Table I. The first item is a natural fluctuation which is due to an intrinsic property of the input temperature T_S, as described by (4). It is assumed here that T_S is due to a steady contribution from the atmosphere, antenna, waveguide, maser, and IF converter. In contrast to this, all other fluctuations are due to imperfections in the radiometer parts. Items 1 through 4 are short-term variations which occur in less than 10 seconds, and items 5 through 9 are additional long-term variations which occur in periods of 30 minutes. The post-detection time constant, τ, in each case is one second. Some promising means for decreasing the fluctuations are also indicated. As can be seen, the observed short-term fluctuation, item 4, is about $2\frac{1}{2}$ times greater than theoretical, item 1, and the total long-term fluctuation is about 10 times greater than theoretical. By increasing τ to 15 seconds, item 4 can be reduced to 0.01°K. This, however, does not greatly reduce the slow

TABLE I—SYSTEM FLUCTUATIONS, τ = 1 sec

Source	Amplitude (rms)	Recommended Improvements
1. Thermal noise	0.015°K (calculated)	Increase the IF bandwidth to coincide with the maser bandwidth
2. Ratio-meter	0.015°K (measured)	Eliminate separate channel gains
3. Noise lamp	0.010°K (estimated)	Synchronize 1-kc switch interval with on excess noise
4. Subtotal of short-term fluctuations	0.040°K (measured)	Increase the post-detection time constant
5. Input waveguide and coaxial line	0.022°K (estimated)	Insulate, and reduce changes in ambient temperature
6. IF converter	0.022°K (calculated)	Use a maser with increased gain, or two masers in series
7. IF gain change	0.001°K (calculated)	Improve B^+ regulation
8. Ratio-meter	0.040°K (estimated)	Eliminate separate channel gains, and improve B^+ regulation
9. Noise lamp pulse circuit	0.025°K (estimated)	Synchronize 1-kc switch interval with on excess noise, and improve B^+ regulation
Total long-term fluctuation (sum of items 4 through 9)	0.150°K (measured)	

fluctuations, items 5 through 9. Thus, for a reasonably long time constant, the total long-term fluctuation will not be reduced much below 0.12°K. The corresponding measured flux density threshold, from (19), for τ = 15 seconds, is

$$\Delta S(\text{measured}) = 1.2 \times 10^{-25} \text{ watts meter}^{-2} \text{ (cps)}^{-1}.$$

With the alterations recommended in Table I, and τ retained at 1 second, it is estimated that the total long-term fluctuation of Table I can be reduced by a factor of 3, to 0.05°K. Using (19)

$$\Delta S(\text{predicted}) = 5 \times 10^{-26} \text{ watts meter}^{-2} \text{ (cps)}^{-1}.$$

XII. EXPERIMENTAL RESULTS

A Crawford Hill sky-plus-environment temperature map was constructed from data taken during an 8-hour period when the sun and moon were below the horizon on Feb. 15, 16, 1961. By avoiding sun and moon temperature anomalies (the sun can add 20°K via side lobes and the moon has been observed to add 16°K via the main beam), it was possible to identify weaker radio sources, including the center of the galaxy, which adds 4.5°K, and delete these from the temperature map.

The raw data consisted of seventeen constant-elevation scans, taken in elevation increments of 1° between −1° and +10°, plus scans at 12°, 15°, 20°, 25° and 30°. A typical scan is shown in Fig. 10. The data were first replotted in terms of system temperature versus elevation for every two degrees of azimuth. With these curves, it was possible to construct a detailed contour map, of which two sample parts are shown in Fig. 11. The absolute accuracy is ±15 per cent, of which ±5 per cent is due to the data-reducing technique and ±10 per cent is due to the temperature calibration accuracy. The latter is discussed in Appendix B.

An elevation scan was made at an azimuth angle of minimum observed temperature, and the results are plotted in Fig. 12. With this curve, it was possible to calculate the absolute value of the zenith sky temperature with good accuracy (see Ref. 1, pages 1088 and 1089), and the result is 2.3 ± 0.2°K. The theoretical value[9] is also plotted and shows good agreement down to an elevation of 1° where the near-side-lobes of the antenna began to intercept the hot earth.

A drift pass of Virgo A, Fig. 13, was obtained by positioning the antenna so the radio source, due to the earth's rotation, would pass through the antenna beam. This, of course, stabilized the side-lobe temperature contributions. At 2390 mc the value of ΔT_s was found to be 1.44°K, and the corresponding flux density, from (19), is 1.48×10^{-24} watts meter^{-2} (cps)$^{-1}$. The value of ΔT_s for Cassiopeia A, from a similar measurement, was found to be 14.3°K, and the corresponding flux density is 1.47×10^{-23} watts meter^{-2} (cps)$^{-1}$. No effort was made to correct these numbers for other weak, but possibly significant, sources in the antenna beam. The flux density measurement accuracy is limited to ±15 per cent, of which ±10 per cent is due to a possible error in the temperature calibration, Appendix B, and ±5 per cent is due to an uncertainty in the antenna gain measurement.

XIII. CONCLUSIONS

A noise-adding radiometer has been found to be a convenient practical tool for measuring small absolute system temperatures over long periods of time. It is compatible with an ultra-low-noise communications receiver, and can be used to check the boresighting of a satellite communications antenna by tracking radio stars.[12] Although the short-term (10-second) system fluctuation is larger than theory by a factor of only $2\frac{1}{2}$ when $\tau = 1$ second, the long-term (30-minute) fluctuation, which limits the minimum detectable power density, is larger than theory by a factor of 10. The sources of excess fluctuation have been identified, and

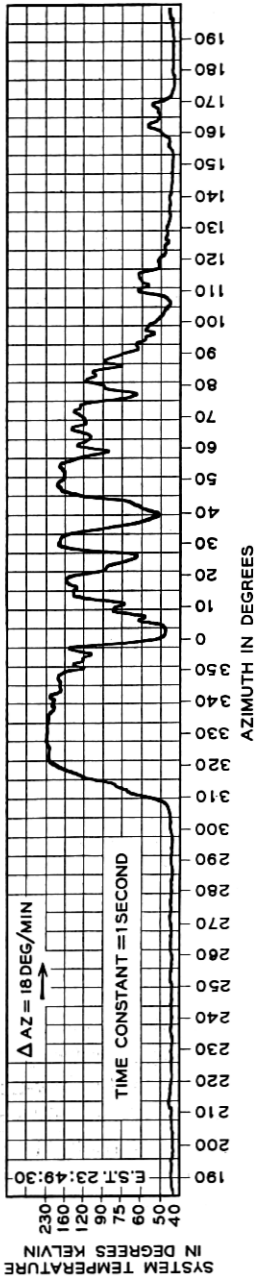

Fig. 10 — System temperature at a 5° elevation.

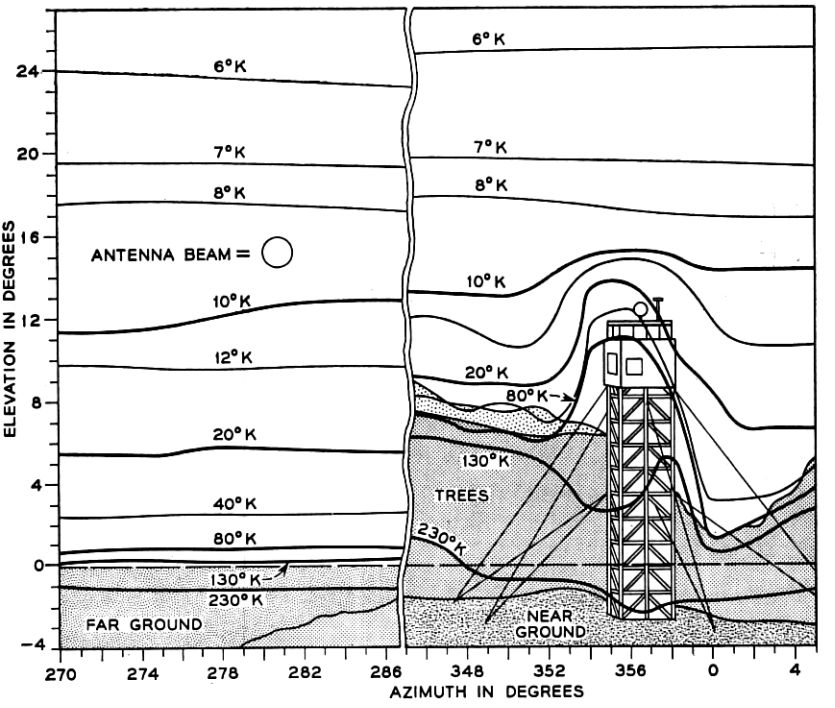

Fig. 11 — Typical environment temperatures of the horn-reflector antenna site at Crawford Hill, N. J. Frequency = 2390 mc; antenna beamwidth = 1.25 degrees.

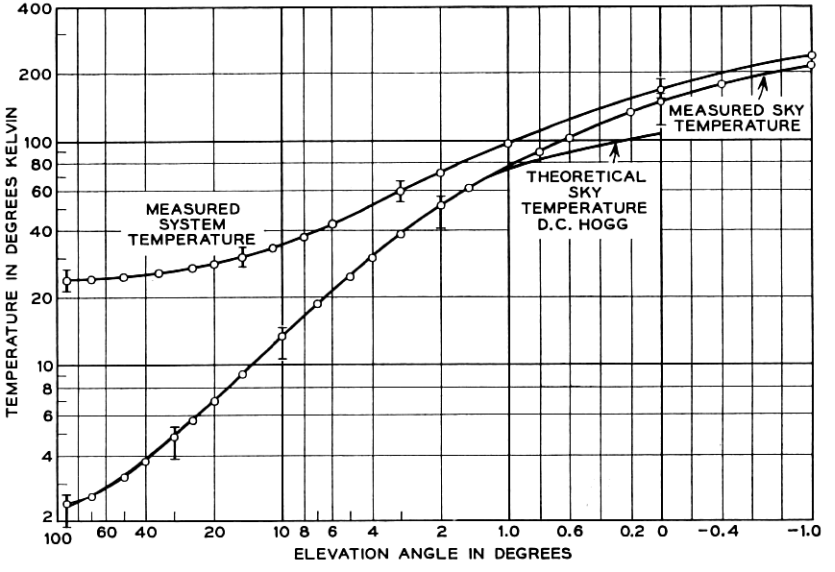

Fig. 12 — Measured sky and system temperatures. Frequency = 2390 mc; azimuth = 190°; time pre-sunrise, February 16, 1961.

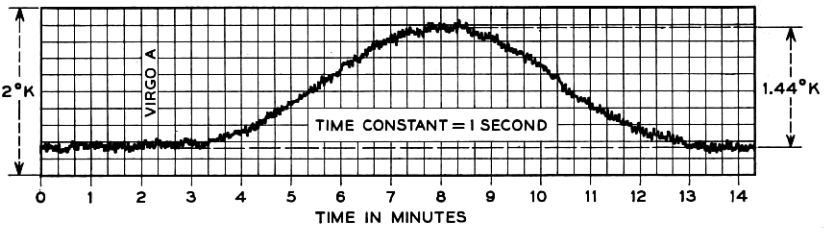

Fig. 13 — Drift pass of Virgo A.

with the suggested alterations, it is believed that the total long-term fluctuation, for $\tau = 1$ second and $B = 16$ mc, can be reduced to 0.05°K, which is larger than theory by a factor of 5.

XIV. ACKNOWLEDGMENTS

The authors are indebted to A. A. Penzias for reducing some sources of receiver fluctuation and to L. H. Enloe for proving the assumptions used in deriving the threshold equation. The authors are also pleased to acknowledge the aid rendered by R. A. Desmond in assembling the noise lamp pulse circuit and the help given by L. Meyers in plotting the data for the environment temperature map.

APPENDIX A

The Minimum Detectable Change in Input Temperature

In the system of Fig. 1, the 1-kc input voltages required by the ratio-meter are derived from the waveforms shown in Fig. 2. From inspection, the voltage switched to each channel has a strong 1-kc component of different amplitude and a small fluctuation due to the input temperature. It is also apparent, but not shown, that a small increase in the system temperature, ΔT_s, will increase each 1-kc component the same amount.

With these inputs, the output of the ratio-meter is a dc voltage on which is superimposed a small fluctuation due to noise. In addition, a slow variation in the dc voltage will occur as in Fig. 13 when noise power received by the antenna increases the system temperature. The theoretical threshold sensitivity will be found by calculating the change of input temperature which causes the dc output voltage to change the same amount as the rms value of the output noise fluctuation.

An examination of the ratio-meter theory of operation[7] shows that the output voltage, V_{out}, is a linear function of the phase angles, φ', which

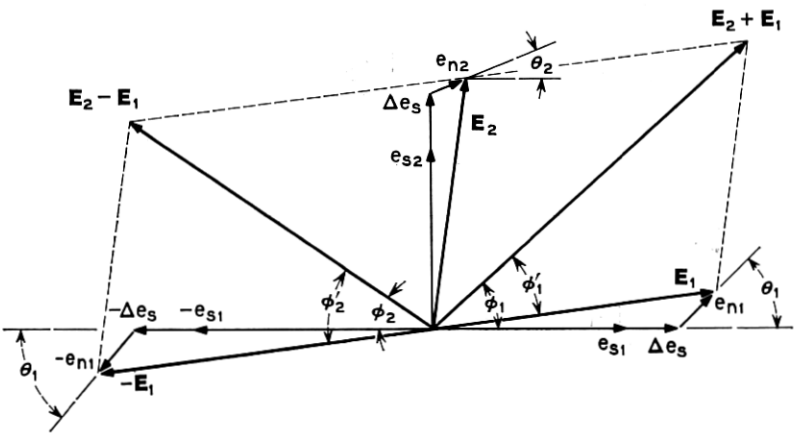

Fig. 14 — Typical ratio-meter input voltages.

result from the vector addition of the input voltages at and around 1 kc. In particular

$$V_{\text{out}} = K\, 2(\varphi_1' + \varphi_2')$$

where K is an arbitrary constant and φ_1' and φ_2' are shown in Fig. 14. Note from the geometry that $\varphi_1' + \varphi_2' = \varphi_1 + \varphi_2$, and therefore V_{out} can also be written

$$V_{\text{out}} = K\, 2\, (\varphi_1 + \varphi_2). \tag{30}$$

As shown in Fig. 14, φ_1 and φ_2 are functions of the input voltages, $\mathbf{E}_1$ and $\mathbf{E}_2$, each of which consists of three parts.

$$\mathbf{E}_1 = e_{S1} + \Delta e_S + \mathbf{e}_{n1}$$

$$\mathbf{E}_2 = e_{S2} + \Delta e_S + \mathbf{e}_{n2}$$

where: e_{S1} = the 1-kc component in channel 1 due to on-off modulation of the input temperature, $T_S + T_A$.

e_{S2} = the 1-kc component in channel 2 due to on-off modulation of the input temperature, T_S.

Δe_S = an in-phase change in the 1-kc components due to a change in input temperature, ΔT_S.

$\mathbf{e}_{n1}$ = a random fluctuation in channel 1 due to the input temperature, $T_S + T_A$.

$\mathbf{e}_{n2}$ = a random fluctuation in channel 2 due to the input temperature, T_S.

From Fig. 14 it can also be seen that

$$\varphi_1 = \tan^{-1}\left(\frac{e_{S2} + \Delta e_S + e_{n2}\sin\theta_2 + e_{n1}\sin\theta_1}{e_{S1} + \Delta e_S + e_{n2}\cos\theta_2 + e_{n1}\cos\theta_1}\right) \tag{31}$$

$$\varphi_2 = \tan^{-1}\left(\frac{e_{S2} + \Delta e_S + e_{n2}\sin\theta_2 - e_{n1}\sin\theta_1}{e_{S1} + \Delta e_S - e_{n2}\cos\theta_2 + e_{n1}\cos\theta_1}\right). \tag{32}$$

Since Δe_S, e_{n1}, and e_{n2} are small compared to e_{S1} and e_{S2}, (31) and (32) can be written:

$$\varphi_1 = \tan^{-1}\frac{e_{S2}}{e_{S1}}\left[1 + \frac{\Delta e_S}{e_{S2}} - \frac{\Delta e_S}{e_{S1}} + \frac{e_{n2}}{e_{S2}}\sin\theta_2 + \frac{e_{n1}}{e_{S2}}\sin\theta_1 - \frac{e_{n2}}{e_{S1}}\cos\theta_2 - \frac{e_{n1}}{e_{S1}}\cos\theta_1\right] \tag{33}$$

$$\varphi_2 = \tan^{-1}\frac{e_{S2}}{e_{S1}}\left\{1 + \frac{\Delta e_S}{e_{S2}} - \frac{\Delta e_S}{e_{S1}} + \frac{e_{n2}}{e_{S2}}\sin\theta_2 - \frac{e_{n1}}{e_{S2}}\sin\theta_1 + \frac{e_{n2}}{e_{S1}}\cos\theta_2 - \frac{e_{n1}}{e_{S1}}\cos\theta_1\right\}. \tag{34}$$

Using the series expansion for $\tan^{-1}$ and noting with dissimilar brackets the differences in signs of (33) and (34)

$$\varphi_1 = \frac{e_{S2}}{e_{S1}}[1 + \cdots] - \frac{1}{3}\left(\frac{e_{S2}}{e_{S1}}\right)^3[1 + \cdots]^3 + \frac{1}{5}\left(\frac{e_{S2}}{e_{S1}}\right)^5[1 + \cdots]^5 + \cdots$$

$$\varphi_2 = \frac{e_{S2}}{e_{S1}}\{1 + \cdots\} - \frac{1}{3}\left(\frac{e_{S2}}{e_{S1}}\right)^3\{1 + \cdots\}^3 + \frac{1}{5}\left(\frac{e_{S2}}{e_{S1}}\right)^5\{1 + \cdots\}^5 + \cdots.$$

Thus $\varphi_1 + \varphi_2$ for use in (30) is

$$\varphi_1 + \varphi_2 = \frac{e_{S2}}{e_{S1}}([1 + \cdots] + \{1 + \cdots\}) - \frac{1}{3}\left(\frac{e_{S2}}{e_{S1}}\right)^3([1 + \cdots]^3 + \{1 + \cdots\}^3) + \frac{1}{5}\left(\frac{e_{S2}}{e_{S1}}\right)^5([1 + \cdots]^5 + \{1 + \cdots\}^5) - \frac{1}{7}\left(\frac{e_{S2}}{e_{S1}}\right)^7([1 + \cdots]^7 + \{1 + \cdots\}^7) + \cdots$$

The first term of $\varphi_1 + \varphi_2$ reduces to

$$+\frac{2e_{S2}}{e_{S1}}\left(1 + \frac{\Delta e_S}{e_{S2}} - \frac{\Delta e_S}{e_{S1}} + \frac{e_{n2}}{e_{S2}}\sin\theta_2 - \frac{e_{n1}}{e_{S1}}\cos\theta_1\right).$$

The second term reduces to

$$-2\left(\frac{e_{S2}}{e_{S1}}\right)^3\left(\frac{1}{3}+\frac{\Delta e_S}{e_{S2}}-\frac{\Delta e_S}{e_{S1}}+\frac{e_{n2}}{e_{S2}}\sin\theta_2-\frac{e_{n1}}{e_{S1}}\cos\theta_1\right).$$

The third term reduces to

$$+2\left(\frac{e_{S2}}{e_{S1}}\right)^5\left(\frac{1}{5}+\frac{\Delta e_S}{e_{S2}}-\frac{\Delta e_S}{e_{S1}}+\frac{e_{n2}}{e_{S2}}\sin\ell_2-\frac{e_{n1}}{e_{S1}}\cos\theta_1\right), \text{ etc.}$$

Therefore $\varphi_1+\varphi_2$ can be written

$$\begin{aligned}\varphi_1+\varphi_2 = {} & 2\left[\frac{e_{S2}}{e_{S1}}-\frac{1}{3}\left(\frac{e_{S2}}{e_{S1}}\right)^3+\frac{1}{5}\left(\frac{e_{S2}}{e_{S1}}\right)^5-\cdots\right] \\ & +2\left[\frac{e_{S2}}{e_{S1}}-\left(\frac{e_{S2}}{e_{S1}}\right)^3+\left(\frac{e_{S2}}{e_{S1}}\right)^5-\cdots\right]\left[\frac{\Delta e_S}{e_{S2}}-\frac{\Delta e_S}{e_{S1}}\right. \\ & \left.+\frac{e_{n2}}{e_{S2}}\sin\theta_2-\frac{e_{n1}}{e_{S1}}\cos\theta_1\right].\end{aligned} \tag{35}$$

The first bracket of (35) is the series expansion of $\tan^{-1}(e_{S2}/e_{S1})$. Thus, it is equal to the rest angle, φ_0, which would result from (31) or (32) if the perturbation terms were zero. The first term is accordingly $2\varphi_0$. The coefficient of the second term of (35) can be written

$$\begin{aligned}2\frac{e_{S2}}{e_{S1}}\left[1-\left(\frac{e_{S2}}{e_{S1}}\right)^2+\left(\frac{e_{S2}}{e_{S1}}\right)^4-\cdots\right] &= \frac{2(e_{S2}/e_{S1})}{1+(e_{S2}/e_{S1})^2} \\ &= \frac{2(e_{S2}/e_{S1})}{\sqrt{1+(e_{S2}/e_{S1})^2}}\cdot\frac{1}{\sqrt{1+(e_{S2}/e_{S1})^2}}.\end{aligned}$$

Since $\varphi_0=\tan^{-1}(e_{S2}/e_{S1})$, it follows from trig identities that this is equivalent to

$$2\sin\varphi_0\cos\varphi_0=\sin 2\varphi_0$$

Thus (35) reduces to

$$\varphi_1+\varphi_2=2\varphi_0+\sin 2\varphi_0\left[\frac{\Delta e_S}{e_{S2}}-\frac{\Delta e_S}{e_{S1}}+\frac{e_{n2}}{e_{S2}}\sin\theta_2-\frac{e_{n1}}{e_{S1}}\cos\theta_1\right].$$

Upon substitution in (30), the output voltage of the ratio-meter is given by

$$V_{\text{out}}=K\left\{4\varphi_0+2\sin 2\varphi_0\left[\frac{\Delta e_S}{e_{S2}}-\frac{\Delta e_S}{e_{S1}}+\frac{e_{n2}}{e_{S2}}\sin\ell_2-\frac{e_{n1}}{e_{S1}}\cos\theta_1\right]\right\} \tag{36}$$

where: $\varphi_0=\tan^{-1}(e_{S2}/e_{S1})$.

Since the detector in Fig. 1 has a square-law characteristic, the 1-kc voltage components, e_{S2} and e_{S1}, at the output of the 1-kc switch assembly, are proportional to the input temperatures $T_S + T_A$ and T_S as indicated in Fig. 2. Therefore φ_0 is a function of the temperature, T_A, added by the noise lamp

$$\varphi_0 = \tan^{-1} \frac{e_{S2}}{e_{S1}} = \tan^{-1} \frac{T_S}{T_S + T_A} = \tan^{-1} (1/Y). \tag{37}$$

Although V_{out} of (36) is thus a function of φ_0, note that the signal component, due to Δe_S, and the noise component, due to e_{n1} and e_{n2}, are both proportional to sin $2\varphi_0$. Thus the theoretical signal-to-noise ratio is independent of φ_0, and a value of φ_0 less than 45° (typically 12°) merely reduces the signal and noise gain by a factor of (0.4). Incidentally, since only the in-phase components of the noise voltages of Fig. 16 are retained in (36), it can be seen that the output of the ratio-meter responds only to the instantaneous in-phase components of the input voltage amplitudes.

In order to determine the threshold sensitivity from (36), e_{S2}, e_{S1}, Δe_S, e_{n2}, and e_{n1} can be calculated using random noise theory. In particular, since the spectral density of the output of a square law detector with a stationary input of white noise is known,[10] and the correlation time corresponding to the large predetection bandwidth is very small compared to each switched interval, the steady and fluctuating parts of $\mathbf{E}_2$ can be calculated by (*i*) assuming the spectral density of the square-law detector input and output is constant with time and (*ii*) allowing the output of the square-law detector to be switched on and off at a 1-kc rate. Similarly, the steady and fluctuating parts of $\mathbf{E}_1$ can be calculated by assuming a larger constant spectral density, which corresponds to the input temperature when the noise lamp is on. An important consequence of the small correlation time is the noise components $\mathbf{e}_{n1}$ and $\mathbf{e}_{n2}$ are uncorrelated, and thus can be added on a power basis. A more rigorous analysis by L. H. Enloe[11] proves these assumptions and arrives at the same result.

The result of switching (or multiplying) the output of the square-law detector with a 1-kc switch can be readily calculated, since these functions are statistically independent, by convolving the spectra density of the square law detector output with that of the 1-kc switch.

$$S_z(f) = \int_{-\infty}^{+\infty} S_x(\psi)\, S_y(f - \psi)\, d\psi \tag{38}$$

where $S_z(f)$ = output spectral density at frequency f
$S_x(f)$ = spectral density of the 1-kc switch = $\frac{1}{4}$ at dc, $1/\pi^2$ at ± 1 kc, $\frac{1}{9}\pi^2$ at ± 3 kc, $\frac{1}{25}\pi^2$ at ± 5 kc, etc.
$S_y(f)$ = spectral density of the square-law detector output = $4a^2A^2B^2$ at dc + $4a^2A^2(B - |f|)$ where $0 < |f| < B$
a = a scaling constant of the square-law detector
A = input spectral density of the square-law detector
B = IF bandwidth.
} From Ref. 10

Since (*i*) the IF bandwidth, $B = 7.75$ mc, is large compared to the switching frequency, $f_0 = 1$ kc, (*ii*) the switch is followed by a bandpass filter of $f_{BP} = f_0 \pm \Delta f/2$, and (*iii*) the switch has a discrete spectral density, (38) reduces to one term for the signal power density at $f_0 = 1$ kc and to a closed series for the bandpass noise power density at $f_0 = 1$ kc.

$$S_z(f_0)\Big|_{\text{signal}} = 2 \times \frac{1}{\pi^2} \times 4a^2A^2B^2 \tag{39}$$

$$S_z(f_0)\Big|_{\text{noise}} = 2 \times 4a^2A^2B\left[\frac{1}{4} + \frac{2}{\pi^2} + \frac{2}{9\pi^2} + \frac{2}{25\pi^2} + \cdots\right]$$

$$S_z(f_0)\Big|_{\text{noise}} = 2a^2A^2B\left[1 + \frac{8}{\pi^2}\left(1 + \frac{1}{9} + \frac{1}{25} + \cdots\right)\right]$$

therefore

$$S_z(f_0)\Big|_{\text{noise}} = 4a^2A^2B. \tag{40}$$

Since $B \gg f_0$, the noise power density of a frequency near f_0 is equal to that at f_0, and is thus equal to that given by (40). The ratio-meter also acts as a frequency converter in that the bandpass noise power densities are converted to frequencies near dc. For example, the noise power density at $f = f_0 + f_1$ and $f = f_0 - f_1$ (where $0 < f_1 < \Delta f/2$) are both converted to the frequency f_1. Since the noise power densities are equal and uncorrelated, the resultant noise power density at f_1 is doubled.

$$S_z(f_1)\Big|_{\substack{\text{converted}\\ \text{noise}}} = 2S_z(f_0)\Big|_{\text{noise}} = 8a^2A^2B. \tag{41}$$

The total noise power in the converted band, when limited by the band-pass filter bandwidth, Δf, is the noise power density of (41) times the range of f_1, i.e., times $\Delta f/2$.

$$\text{Noise power (limited by } \Delta f) = 4a^2A^2B\Delta f.$$

In order to reduce the output noise further, the ratio-meter is followed by a narrow low-pass filter of bandwidth b (where $b < \Delta f/2$). In this case

$$\text{Noise power (limited by } b) = 8a^2A^2Bb$$

and the corresponding output noise voltage (rms value) is

$$e_n(\text{rms}) = 2\sqrt{2}\, a\, A\sqrt{Bb}. \tag{42}$$

The signal voltage at 1 kc (peak value) is $\sqrt{2}$ times the square root of the spectral density at 1 kc. Therefore, from (39),

$$e_S(\text{peak}) = \frac{4}{\pi}\, a\, AB. \tag{43}$$

and the corresponding change in signal voltage (peak value) is

$$\Delta e_S(\text{peak}) = \frac{4}{\pi}\, a\, B\Delta A. \tag{44}$$

The quantities required by (36) are given by (42), (43), and (44). However, the spectral density, A, at the input of the square-law detector is different for each channel and is proportional to the assumed input temperature; i.e.,

$$\text{if } A_2 = CT_S,$$
$$\text{then } A_1 = C(T_S + T_A);$$
$$\text{therefore } \Delta A_2 = \Delta A_1 = C\Delta T_S.$$

Referring now to (36), the Δe_S terms can be written

$$\frac{\Delta e_S}{e_{S2}} - \frac{\Delta e_S}{e_{S1}} = \frac{\Delta A}{A_2} - \frac{\Delta A}{A_1} = \frac{C\Delta T_S}{CT_S} - \frac{C\Delta T_S}{C(T_S + T_A)} = \frac{\Delta T_S T_A}{(T_S + T_A)T_S}. \tag{45}$$

Since the amplitude and phase of e_{n2} and e_{n1} are random and uncorrelated, the total rms fluctuation due to the noise terms can be found by

adding the individual rms values on a power basis:

$$\frac{e_{n2}}{e_{s2}} \sin \theta_2 - \frac{e_{n1}}{e_{s1}} \cos \theta_1 = \left\{ \left[\frac{e_{n2}}{\sqrt{2}\, e_{s2}} \right]^2 + \left[\frac{e_{n1}}{\sqrt{2}\, e_{s1}} \right]^2 \right\}^{\frac{1}{2}}$$

$$= \left\{ \left[\frac{e_{n2}(\text{rms})}{e_{s2}(\text{peak})} \right]^2 + \left[\frac{e_{n1}(\text{rms})}{e_{s1}(\text{peak})} \right]^2 \right\}^{\frac{1}{2}} = \left\{ \left[\frac{\pi}{\sqrt{2}} \sqrt{\frac{b}{B}} \right]^2 + \left[\frac{\pi}{\sqrt{2}} \sqrt{\frac{b}{B}} \right]^2 \right\}^{\frac{1}{2}} = \pi \sqrt{\frac{b}{B}}. \tag{46}$$

Inserting (45) and (46) into (36)

$$V_{\text{out}} = K \left\{ 4\varphi_0 + 2 \sin 2\varphi_0 \left[\frac{\Delta T_S T_A}{(T_S + T_A) T_S} + \pi \sqrt{\frac{b}{B}} \right] \right\} \tag{47}$$

where: $\varphi_0 = \tan^{-1} (e_{s2}/e_{s1}) = \tan^{-1} (1/Y)$.

The second-from-last term is due to a change, ΔT_S, of input temperature, and the last term is an rms variation due to noise fluctuations. The minimum detectable change of input temperature can be found by equating the last two terms. The result is

$$\Delta T_S(\text{theoretical}) = T_S \left(1 + \frac{T_S}{T_A} \right) \pi \sqrt{\frac{b}{B}}. \tag{48}$$

It can be shown that the noise bandwidth, b, of an RC low-pass filter is equal to $\frac{1}{4}$ RC $= \frac{1}{4}\tau$ where τ is the RC time constant. With this substitution (48) becomes

$$\Delta T_S(\text{theoretical}) = T_S \left(1 + \frac{T_S}{T_A} \right) \frac{\pi}{2} \frac{1}{\sqrt{B\tau}}. \tag{49}$$

APPENDIX B

Calibration

Since Y is the ratio of two noise powers, the output voltage of the radiometer can be calibrated well in advance without using the antenna or maser preamplifier. To do this, the coaxial noise lamp is connected to the input of the IF converter via an RF level-set attenuator. Since the converter noise temperature is about 1350°K and the excess noise temperature of a coaxial noise lamp is about 8360°K, a value of $Y \approx 5.5$ can be obtained. By adjusting the level set attenuator this can be varied down to $Y \approx 1$. The resulting value of Y is measured precisely by noting the change of IF attenuation required to keep the IF output power constant when the noise lamp is turned on. By pulsing the lamp

at a 1-kc rate, the corresponding ratio-meter output voltage can be measured with the precision dc voltmeter. Although the effective value of Y under pulsing conditions may be somewhat less due to ionization and deionization effects, the above method of calibration bypasses this as a source of error. The accuracy of the resulting Y versus V curve, Fig. 7, is limited by (*i*) the precision IF attenuator, to ± 3.0 per cent, and (*ii*) the precision dc voltmeter, to ± 1.0 per cent, for a subtotal of ± 4.0 per cent. Since the T_S versus V curve, Fig. 7, is, in addition, a function of T_A, (2), and the accuracy of T_A, for $T_A = 94.6°K$, is limited by (*iii*) the noise lamp temperature, to ± 2.7 per cent, and (*iv*) the directional coupling, to ± 3.6 per cent, for a subtotal of ± 6.3 per cent, the total accuracy of the absolute system temperature calibration is ± 10.3 per cent.

REFERENCES

1. Ohm, E. A., Project Echo Receiving System, B.S.T.J., **40**, July, 1961, p. 1065.
2. DeGrasse, R. W., Hogg, D. C., Scovil, H. E. D., and Ohm, E. A., Ultra-Low-Noise Antenna and Receiver Combination for Satellite or Space Communication, Proc. Nat. Elec. Conf., **15**, Oct., 1959, p. 370.
3. Dicke, R. H., The Measurement of Thermal Radiation at Microwave Frequencies, Rev. Sci. Instr., **17**, July, 1946, p. 268.
4. Selove, W., A DC Comparison Radiometer, Rev. Sci. Instr., **25**, Feb., 1954, p. 120.
5. Crawford, A. B., Hogg, D. C., and Hunt, L. E., A Horn-Reflector Antenna for Space Communications, B.S.T.J., **40**, July, 1961, p. 1107.
6. DeGrasse, R. W., Kostelnick, J. J., and Scovil, H. E. D., The Dual Channel 2390-mc Traveling-Wave Maser, B.S.T.J., **40**, July, 1961, p. 1125.
7. 416A/AR Ratio Meter Operating and Servicing Manual, Hewlett-Packard Co., Nov., 1959, Section III.
8. Kuhn, N. J., and Negrete, M. R., Gas Discharge Noise Sources in Pulsed Operation, I.R.E. International Convention Record, Part 3, Mar., 1961, p. 166.
9. Hogg, D. C., Effective Antenna Temperatures Due to Oxygen and Water Vapor in the Atmosphere, J. Appl. Phys., **30**, Sept., 1959, p. 1417.
10. Davenport, W. B., Jr., and Root, W. L., *Random Signals and Noise*, McGraw-Hill, New York, 1958, p. 256.
11. Enloe, L. H., Sensitivity of a Noise-Adding Radiometer, private communication, Nov. 5, 1962.
12. Jakes, W. C., and Penzias, A. A., unpublished work.